Detection of Ultrafast Phenomena Using a Modified Sagnac Interferometer

David H. Hurley and Oliver B. Wright

Department of Applied Physics
Faculty of Engineering
Hokkaido University
Sapporo, JAPAN 060-8628,

Abstract:

We describe a time division interferometer based on the Sagnac geometry for monitoring ultrafast changes in the real and imaginary components of refractive index as well as phase changes due to surface displacement. Particular advantages are its simple common path design and the ease of obtaining high spatial resolution by tight focusing at normal incidence with a single microscope objective for both pumping and probing. The operation is demonstrated by the detection of temperature changes and coherent phonon generation in a gold film.

Introduction:

As femtosecond lasers become more compact and cheaper the need for vibration insensitive and robust measurement methods is increasing. The time resolved measurement of ultrafast changes in refractive index and surface motion is a subject of extensive interest because of its wide application to the study of light-matter interactions. Interferometric techniques in particular have proved useful for studying phenomena as diverse as femtosecond plasma diagnostics [1], ultrafast optical switching [2] or picosecond optoacoustics [3,4] because of their sensitivity, relative simplicity and ability to resolve both phase and amplitude changes to a probe pulse. All these techniques rely on the interference between a probe pulse (that arrives at the sample after a pump pulse) and a reference pulse (that arrives before). Two representative linear interferometric techniques that are used together with optical pumping and probing are spectral interferometry [1, 5] and time division interferometry (TDI) [2, 6]. The former has the advantage of not requiring active stabilization, but does require a spectrometer system combined with complex signal processing. The latter is simpler in principle, but all designs published so far, based on Mach Zehnder or Michelson geometries, require active stabilization for long term operation; this TDI technique is particularly suited to the study of small perturbative changes to the refractive index. To our knowledge none of such interferometric methods proposed are fully common path, in that they require probe and reference pulses to travel separate routes for some of their trajectory, rendering such interferometers more sensitive to parasitic fluctuations from thermal and acoustic fields.

In this Letter we describe a simple common path time division interferometer for monitoring ultrafast changes in refractive index in reflection mode at normal incidence. The use of normal incidence facilitates the use of powerful microscope objectives in order to achieve high spatial resolution (~1 μm), and allows the same lens to be used for pumping and probing. We demonstrate its operation by the detection of ultrashort time scale transient temperature changes and coherent phonon propagation in a gold film.

The interferometer, shown in Fig. 1, is based on a Sagnac design. The pump and probe pulses are derived from the same laser (as described in more detail later). The input polarization to the interferometer is oriented at 45° to the x and y axes as shown. The non-polarizing beam splitter (NPBS) directs a portion of the probe beam into photodetector b to act as a laser intensity sampling beam in a standard differential detection scheme. The remaining half of the input beam is split into

vertical and horizontal polarizations, the probe and reference beams, respectively, by the first PBS. The beams are recombined at the second PBS and directed through a $\lambda/4$ plate (aligned with axes at 45° to the x and y axes). Both beams are focused by a lens at normal incidence onto the sample. On reflection they are transmitted a second time through the waveplate, reverse paths, and are then combined again at the first PBS. Half of this interferometric beam is directed through another $\lambda/4$ plate and then through a polarizer to photodetector via the NPBS. The probe and reference beams spatially overlap, but have opposite polarizations and interfere with the aid of the polarizer. Apart from the picosecond-order time separation between the probe and reference pulses while passing through the PBS and sample section of the interferometer, these pulses experience identical optical paths.

The characteristics of the interferometer are easily calculated using Jones calculus. After traveling identical paths through the sample section of the interferometer, the polarization state of the composite beam upon reflection by the NPBS can be expressed as $E_1\hat{\mathbf{x}} + E_2\hat{\mathbf{y}}$, where $\hat{\mathbf{x}}$ and $\hat{\mathbf{y}}$ are unit vectors, and E_1 and E_2 represent the probe and reference beams, respectively (with normal
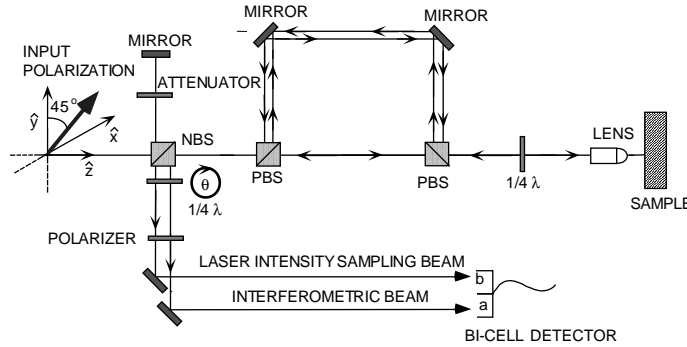

Fig.1 Modified Sagnac interferometer. The 1/4 wave plate and polarizer combination are used to achieve maxium phase sensitivity.

operation at $E_1=E_2$). The coordinate system is chosen such that z is always the beam propagation direction and y is the upward vertical direction. The composite beam is then directed through a $\lambda/4$ wave plate and a linear polarizer with the transmission axis aligned along the $\hat{\mathbf{x}} - \hat{\mathbf{y}}$ direction. The intensity falling on the photodetector can be expressed as $I = ((r'A_1)^2 + (rA_2)^2)(1 - M\cos(\theta_2 - \theta_1))$, where

$$A_{1/2} = E_{1/2}\sqrt{\mp\cos^2(\psi)\sin(\psi)\pm\sin(\psi)/2 + 1/4},$$
$$\theta_{1/2} = \pm\arctan\left(1 - 2\cos^2(\psi)\pm 2\sin(\psi)\cos(\psi)\right), \qquad (1)$$
$$M = 2A_1A_2/(A_1^2 + A_2^2).$$

The complex amplitude reflection coefficient of the sample seen by the reference pulse is expressed as r while $r'=r'(\tau)$ is used to express the reflection coefficient of the probe pulse, τ the delay time between the pump and probe pulses [7]. (Strictly r' represents an average over the optical probe pulse duration.) The interferometer characteristics as a function of the angle ψ are

illustrated in Fig. 2. We show (for the case $|r|=|r'|$ and $E_1=E_2$) a) the phase difference θ between the reference and probe components of the electric field after transmission through the $\lambda/4$ plate, b) the fringe visibility or interferometer modulation, and c) the total intensity at the photodetector. The maximum interferometric sensitivity, fringe visibility and intensity at the detector are simultaneously achieved with $\psi=0^o$, 90°, 180°, and 270°. Zeros in intensity occur half way between these values, providing a check on the interferometer alignment.
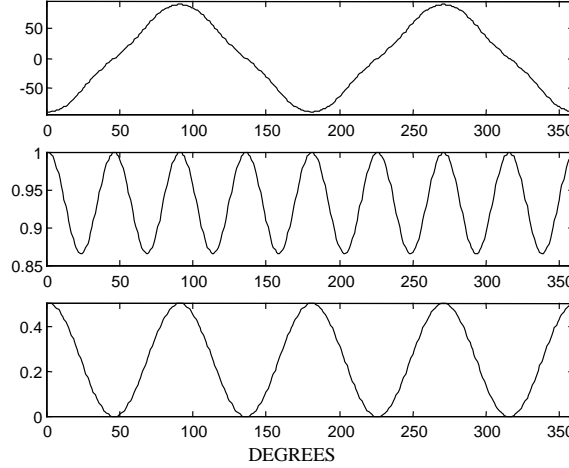

Fig. 2. Top: Phase difference in degrees between the reference and the probe after transmission through the polarizer, Middle: Fringe visibility, and Botttom: total intensity at the photodetector normalized to that before the polarizer, plotted as a function of the angle of the second 1/4 wave plate.

For application to the ultrafast measurement of the real and imaginary changes in reflectance $\delta r=r'-r$, simple data manipulation of data records taken at $\psi=0^o$ and 90° is sufficient. The experiments in this Letter concern small changes in reflectance, and it is convenient to write r $=r_0\exp[i\phi_0]$ and $r'=r_0(1+\rho)\exp[i(\phi_0+\delta\phi)]$, where ρ ($\ll 1$) is the relative change in reflectance and $\delta\phi$ ($\ll 1$) is the change in phase induced by the pump pulse ($\delta r/r \bullet \rho+i\delta\phi$). Both ρ and $\delta\phi$ are functions of τ. With these definitions, Eq. (1) implies that the $\psi=0^o$ and $\psi=90^o$ outputs of the photodetector are proportional to:

$$I_0 \approx (E_1^{\ 2} + E_2^{\ 2})r_0^{\ 2} + 2r_0^{\ 2}E_1^{\ 2}\rho - 2r_0^{\ 2}E_1E_2\delta\phi \,, \tag{2}$$

$$I_{90} \approx (E_1^{\ 2} + E_2^{\ 2})r_0^{\ 2} + 2r_0^{\ 2}E_1^{\ 2}\rho + 2r_0^{\ 2}E_1E_2\delta\phi \,, \tag{3}$$

respectively. The sum and difference of these two equations can therefore be used to extract ρ and $\delta\phi$ [4]. Although we have not done so it would be possible to monitor I_0 and I_{90} simultaneously by splitting the beam reflected from the NPBS into two by means of an extra beam splitter, and using twin waveplates, polarizers and detectors.

As a check on the experimental technique, the reflectivity response ($\delta R/R \bullet 2\rho$, for $\rho \ll 1$) can be obtained separately by rotating the first $\lambda/4$ plate by 45°. The probe and reference beams then traverse different paths inside the interferometer, do not overlap temporally and do not interfere. The intensity at the photodiode then takes the form, for $\psi=0$, 45°, 90°... and with the same scale factor as in Eqs. (2)-(3),

$$I_R \approx (E_1{}^2 + E_2{}^2)r_0{}^2 + 2E_1{}^2 r_0{}^2 \rho. \tag{4}$$

We have tested the interferometer with experiments to examine the short time thermoelastic response of a gold film. The initial proposals by Eesley *et al.* and Thomsen *et al.* to respectively detect temperature changes and coherent phonons in opaque thin films relied on the coupling of the refractive index to temperature and strain [8,9]. Phonon detection from ultrafast surface vibrations was reported a few years later [10]. Our interferometer has great potential in these applications because it allows independent measurements of both reflectance and phase, giving more complete information on the ultrafast response in a configuration convenient for mapping such properties with ~1 μm spatial resolution. The gold film sample of thickness 330 nm was prepared by electron beam deposition on a silica substrate. The pump and probe pulses are derived from the same femtosecond Ti:sapphire laser (Spectra-Physics, Tsunami) with ~100 fs pulse duration (FWHM). The 830 nm output is used for the reference and probe beams, whereas the second harmonic at 415 nm is used for the pump beam. As shown in Fig. 1, these two wavelengths are combined with a dichroic beam splitter to allow all the beams to pass through the same ∞50 microscope objective to produce a ~2 μm diameter spot on the sample. As is common practice, the pump pulse is modulated with an acoustic optic modulator (at ~1 MHz) for lock-in detection of the modulated terms in Eqs. (2)-(4), and a shaker placed before the interferometer provides a variable optical delay. Resolution of intensity fluctuations ~10^{-7} and phase changes ~0.1 μrad are achieved with typically 1000 cycles of the shaker at 8 Hz, with effective sub-100 fs temporal resolution.

Figure 3(a) and (b) show the two interferometric responses (I_0 and I_{90}) for a pump fluence of 1 mJcm^{-2} (and probe fluence 0.2 mJcm^{-2}). The sharp changes in signal near $\tau=0$ are caused by the coupling of the refractive index to the electron gas and lattice temperature [8]. This is followed by two acoustic echoes arising from the reflection of longitudinal coherent phonon pulses from the film-substrate interface. In Fig. 3(c) the reflectance change ρ is plotted together with that measured directly [using Eq. (4)]. The shape of the two curves are in close agreement, showing a gradual decay due to thermoreflectance together with a relatively weak acoustic echo signal arising from piezoreflectance. (The small discrepancy in the overall amplitude is probably due to the probe beam for the direct reflectance measurement taking a slightly different path through the polarizing optics.) The phase signal ϕ in Fig. 3(d) shows enhanced acoustic echoes because the signal includes a contribution from surface motion that is directly related to the shape of the strain pulse in the film [10,11].

The general equation for the optical response of the film is [9]

$$\frac{\delta r}{r} = -2ik_0\delta z + \frac{4ik_0\tilde{n}}{(1-\tilde{n}^2)}\int_0^\infty \left[\left(\frac{dn}{d\eta} + i\frac{d\kappa}{d\eta}\right)\eta(z,t) + \left(\frac{dn}{dT} + i\frac{d\kappa}{dT}\right)T(z,t)\right]\exp(2ik_0z\tilde{n})dz\,, \tag{5}$$

where we have included the effect of the outward surface displacement δz on the phase. Here $\tilde{n} = n+i\kappa$ is the refractive index, $k_0 = 2\pi/\lambda$ is the free space wavevector, and $\eta(z,t)$ and $T(z,t)$ are the temperature and longitudinal strain distributions in the film ($\eta=\eta_{33}$). Although more sophisticated models are available [12], these distributions can be obtained from the coupled diffusion equations for the electron and lattice temperatures, leading, for ~100 fs light pulses in gold in the present fluence regime, to an initial exponential temperature profile varying as $\exp(-\sqrt{(g/\kappa)}\,z)$, where g is the electron-phonon coupling constant and κ is the thermal conductivity [12]. This in turn leads to an expression for the thermoelastic strain $\eta(z,t)$. From the ratio of the components of the measured signal ρ to the signal ϕ, we estimate that the second term in Eq. (5) is $\lesssim 10\%$ of the first. The fit to the phase shown by the curve (ii) in Fig. 4(d) is based on values of g, κ and sound
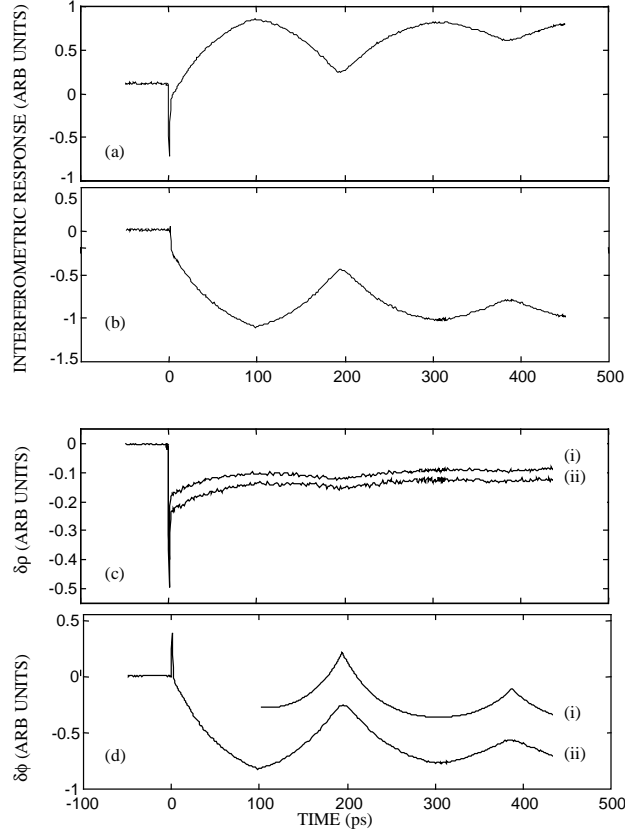
Fig. 3. (a), (b) The interferometric responses for $\psi=0^o$ and $\psi=90^o$ for a gold film as a function of delay time between the pump and probe pulses. (c) Reflectance ρ derived from the interferometric response (i) and from direct measurement (ii). (d) Phase $\delta\phi$ derived from the interferometric response (ii) and theoretical fit to the acoustic echoes (i).

velocities taken from Ref. 11, assuming that this second term is negligible. Good agreement is obtained, demonstrating the effectiveness of the interferometer for quantitative measurements of phonon generation and propagation in gold.

In conclusion, we have described a common path time division interferometer for monitoring ultrafast changes in refractive index and surface motion in reflection mode. This interferometer should find applications in many areas of ultrafast diagnostics of the response of materials to illumination by ultrashort optical pulses.

<u>Acknowledgements</u>

References:

[1] J. P. Geindre *et al.*, Optics Lett. **19**, 1997 (1994); P. Blanc *et al.*, J. Opt. Soc. Am. B **13**, 118 (1996).
[2] L. Sarger *et al.*, J. Opt. Soc. Am. **B 11**, 995 (1994).
[3] O. B. Wright and T. Hyoguchi, Opt. Lett. **16**, 1529-1531 (1991).

[4] B. Perrin, B. Bonello, J. C. Jeannet, E. Romatet, Progress in Natural Science (China) **S6**, 444 (1996); C. J. K. Richardson, M. J. Ehrlich and J. W. Wagner, **Rev. Sci. Instrum**. *JOSA B* (in press).

[5] J. Piasecki. B. Colombeau. M. Vampouille, C. Froehly and J. A. Arnaud, Appl. Opt. 19 3749 (1980); E. Tokunaga, A. Terasaki and T. Kobayashi, Optics Lett. **17**, 1131 (1992); L. Lepetit. G. Cheriaux and M. Joffre, J. Opt. Soc. Am. B **12**, 2467 (1995).

[6] J. M. Halbout and C. L. Tang, Appl. Phys. Lett. **40**, 765 (1982); M. J. LaGasse, K. K. Anderson, H. A. Haus and J. G. Fujimoto, Appl. Phys. Lett. **54**, 2068 (1989).

[7] This expression takes into account the 90° change in polarization direction that occurs on reflection from the NPBS.

[8] G. L. Eesley, Phys. Rev. B **33**, 2144 (1986).

[9] C. Thomsen, H. T. Grahn, H. J. Maris, and J. Tauc, Phys. Rev. B **34**, 4219 (1986).

[10] O. B. Wright and K. Kawashima, Phys. Rev. Lett. **69**, 1668 (1992).

[11] O. B. Wright, Phys. Rev. B **49**, 9985 (1994).

[12] V. E. Gusev and O. B. Wright, Phys. Rev. B **57**, 2878 (1998).

[13] O. B. Wright and V. E. Gusev, IEEE Trans. Ultrason., Ferroelec., Freq. Contr. **42**, 329 (1995).

<u>Figure Captions</u>

Fig. 1: The modified Sagnac interferometer. The $\lambda/4$ plate and polarizer combination are used to achieve maximum phase sensitivity.

Fig. 2: (a) Phase difference between the reference and probe before the polarizer, (b) fringe visibility (interferometer modulation) at the photodetector, and (c) total intensity at the photodetector, plotted as a function of the angle ψ of the second $\lambda/4$ plate.

Fig. 3: (a), (b) The interferometric responses for $\psi=0^o$ and $\psi=90^o$ for a gold film as a function of delay time between the pump and probe pulses. (c) Reflectance ρ derived from the interferometric response (i) and from direct measurement (ii). (d) **Phase $\delta\phi$ derived from the interferometric response (i) and theoretical fit to the acoustic echoes (ii).** *It was more convenient to put theory on top …space considerations. Thus (i) and (ii) must be switched.*